Coupling of a two phase gas liquid 3D Darcy flow in fractured porous media with a 1D free gas flow

Konstantin Brenner, Roland Masson, Laurent Trenty, Yumeng Zhang

Coupling of a two phase gas liquid 3D Darcy flow in fractured porous media with a 1D free gas flow

K. Brenner[*], R. Masson[†], L. Trenty[‡], Y. Zhang[§]

February 1, 2015

Abstract

A model coupling a three dimensional gas liquid compositional Darcy flow in a fractured porous medium, and a one dimensional compositional free gas flow is presented. The coupling conditions at the interface between the gallery and the porous medium account for the molar normal fluxes continuity for each component, the gas liquid thermodynamical equilibrium, the gas pressure continuity and the gas and liquid molar fractions continuity. The fractures are represented as interfaces of codimension one immersed in the surrounding 3D porous medium, the matrix. Pressure continuity is assumed for both phases at the interfaces between the fracture and the matrix. The spatial discretization is based on the Vertex Approximate Gradient (VAG) scheme in the porous medium coupled with a non conforming control volume finite element discretization in the gallery. This model is applied to the simulation of the mass exchanges at the interface between the repository and the ventilation excavated gallery in a nuclear waste geological repository.

1 Introduction

Flow and transport processes in domains composed of a porous medium and an adjacent free-flow region appear in a wide range of industrial and environmental applications. This is in particular the case for radioactive waste deep geological repositories where such models must be used to predict the mass and energy exchanges occuring at the interface between the repository and the ventilation excavated galleries. Typically, in this example, the porous medium initially saturated with the liquid phase is dried by suction in the neighbourhood of the interface. To model such physical processes, one needs to account in the porous medium for the flow of the liquid and gas phases including the vaporization of the water component in the gas phase and the dissolution of the gaseous component in the liquid phase. In the gallery, a single phase gas free flow can be considered assuming that the liquid phase is instantanneously vaporized at the interface. This single phase gas free flow has to be compositional to account for the change

[*]Laboratoire de Mathématiques J.A. Dieudonné, UMR 7351 CNRS, University Nice Sophia Antipolis, and team COFFEE, INRIA Sophia Antipolis Méditerranée, Parc Valrose 06108 Nice Cedex 02, France, konstantin.brenner@unice.fr

[†]Laboratoire de Mathématiques J.A. Dieudonné, UMR 7351 CNRS, University Nice Sophia Antipolis, and team COFFEE, INRIA Sophia Antipolis Méditerranée, Parc Valrose 06108 Nice Cedex 02, France, roland.masson@unice.fr

[‡]Andra, 1-7 rue Jean Monnet 92290 Chatenay-Malabry, France, laurent.trenty@andra.fr

[§]Laboratoire de Mathématiques J.A. Dieudonné, UMR 7351 CNRS, University Nice Sophia Antipolis, and team COFFEE, INRIA Sophia Antipolis Méditerranée, Parc Valrose 06108 Nice Cedex 02, France, yumeng.zhang@unice.fr

of the relative humidity in the gallery which has a strong feedback on the liquid flow rate at the interface.

In this work we consider a reduced model coupling a gas liquid Darcy flow in the porous medium with a 1D free flow in the gallery. It assumes that the longitudinal dimension of the gallery is large compared with its diameter. The liquid and gas phases are considered as a mixture of two components, the water component denoted by e which can vaporize in the gas phase, and the gaseous component a standing for air which can dissolve in the liquid phase. The matching conditions at the porous medium gallery interface are a simplified version of those proposed in [13, 3] taking into account the low permeability of the repository. In this case, it can be assumed that the gas pressure, and the gas molar fractions are both continuous at the interface. In addition, following [13, 3], the thermodynamical equilibrium between the gas and liquid phases is assumed to hold at the interface.

The flow in the porous medium takes into account the mass exchanges between a network of discrete fractures and the surrounding 3D porous medium, the matrix. Following [1] we consider the asymptotic model for which the fractures are represented as interfaces of codimension one immersed in the matrix domain. The pressures at the interfaces between the matrix and the fracture network are assumed continuous corresponding to a large ratio between the normal permeability of the fracture and the width of the fracture compared with the ratio between the permeability of the matrix and the size of the domain. The extension of such model to two phase Darcy flows is analysed in [5] and assumes that both phase pressures are continuous at the matrix fracture interfaces.

The coupled model is formulated in terms of a single set of unknowns used in the matrix, in the fracture network and in the gallery corresponding to the liquid and gas pressures. Its discretization is based on the Vertex Approximated Gradient (VAG) scheme introduced in [10] for the single phase Darcy flow, in [8] for compositional Darcy flows, and in [5] for two phase Darcy flows in discrete fracture networks. The VAG scheme is roughly speaking a finite volume nodal approximation. Its main advantage compared with typical nodal finite volume schemes such as Control Volume Finite Element (CVFE) methods [3] is to avoid the mixing of different material properties inside the control volumes. This idea is here extended to take into account the coupling with the 1D free gas flow using a 1D finite element mesh non necessarily matching with the porous medium mesh.

The outline of the article is the following: section 2 details our reduced 3D-2D-1D coupled model and its formulation using a single set of unknowns corresponding to the gas and liquid pressures. In section 3, the VAG discretisation is extended to our coupled model. Then, section 4 exhibits the numerical results obtained on two examples including 1 and 4 fractures.

2 Coupled Model

Let ω and $S \subset \omega$ be two simply connected polygonal domains of $\mathbb{R}^2$ and $\Omega = (0, L) \times (\omega \setminus \overline{S})$ be the cylindrical domain defining the porous medium. The excavated gallery corresponds to the domain $(0, L) \times S$ and it is assumed that the free flow in the gallery depends only on the x coordinate along the gallery and on the time $t \in (0, T_f)$. Let us denote by $\Gamma = (0, L) \times \partial S$ the interface between the gallery and the porous medium and by γ the trace operator from $H^1(\Omega)$ to $L^2(\Gamma)$. We define on Γ the coordinate system (x, s) where s is the curvilinear coordinate along ∂S.

Let $\overline{\Gamma}_f = \bigcup_{i\in I} \overline{\Gamma}_{f_i}$ and its interior $\Gamma_f = \overline{\Gamma}_f \setminus \partial\overline{\Gamma}_f$ denote the network of fractures $\Gamma_{f_i} \subset \Omega$, $i \in I$, such that each Γ_{f_i} is a planar polygonal simply connected open domain included in a plane $\mathcal{P}_i$ of $\mathbb{R}^3$. It is assumed that $\Gamma_f \cap \partial\Omega = \emptyset$ and we denote by Σ the fracture intersections. Let us set $\Sigma_0 = \partial\Gamma_f \cap (\partial\Omega \setminus \overline{\Gamma})$ and $\Sigma_\Gamma = \partial\Gamma_f \cap \overline{\Gamma}$.

Let $\alpha = g, l$ denote the gas and liquid phases assumed to be both defined by a mixture of two components, the water component denoted by e which can vaporize in the gas phase, and the gaseous component a standing for air which can dissolve in the liquid phase. Following [4] (see also [12] for the case of N components), the gas liquid Darcy flow formulation uses the gas pressure p^g and the liquid pressure p^l as primary unknowns, denoted by $\mathbf{u} = (p^g, p^l)$ in the following. In this formulation, the component molar fractions of the gas and liquid phases are defined by some functions $c_i^\alpha(\mathbf{u})$ of the phase pressures such that $c_e^\alpha(\mathbf{u}) + c_a^\alpha(\mathbf{u}) = 1$. Consequently the molar and mass densities, as well as the viscosities can be defined as functions of $\mathbf{u}$ and will be denoted by respectively $\zeta^\alpha(\mathbf{u})$, $\rho^\alpha(\mathbf{u})$, $\mu^\alpha(\mathbf{u})$ for $\alpha = g, l$.

In the matrix domain $\Omega \setminus \overline{\Gamma}_f$ let us use the following notations:

- The saturations are given by the functions $s_m^\alpha(\mathbf{x}, p_c)$ of the capillary pressure $p_c = p^g - p^l$ with $s_m^l(\mathbf{x}, p_c) + s_m^g(\mathbf{x}, p_c) = 1$.
- The relative permeabilities are denoted by $k_{r,m}^\alpha(\mathbf{x}, s^\alpha)$ for $\alpha = g, l$.
- The porosity is denoted by $\phi_m(\mathbf{x})$, and the permeability tensor by $\mathbf{K}_m(\mathbf{x})$

Similarly, in the fracture network Γ_f let us use the following notations:

- The saturations are given by the functions $s_f^\alpha(\mathbf{x}, p_c)$ of the capillary pressure with $s_f^l(\mathbf{x}, p_c) + s_f^g(\mathbf{x}, p_c) = 1$.
- The relative permeabilities are denoted by $k_{r,f}^\alpha(\mathbf{x}, s^\alpha)$ for $\alpha = g, l$.
- The porosity is denoted by $\phi_f(\mathbf{x})$, the fracture width by $d_f(\mathbf{x})$, and the tangential permeability tensor by $\mathbf{K}_f(\mathbf{x})$.

Following [5] it is assumed that both phase pressures are continuous at the matrix fracture interfaces such that the pressures in the fracture network are defined by $\gamma_f p^\alpha$ for $\alpha = g, l$ where γ_f denote the trace operator from $H^1(\Omega)$ to $L^2(\Gamma_f)$. Then, the Darcy law in the fracture network is obtained by the reduced model

$$\mathbf{V}_f^\alpha = -\frac{k_{r,f}^\alpha(\mathbf{x}, s_f^\alpha(\gamma_f(p^g - p^l)))}{\mu^\alpha(\gamma_f \mathbf{u})} d_f(\mathbf{x}) \mathbf{K}_f(\mathbf{x}) \Big(\nabla_\tau \gamma_f p^\alpha - \rho^\alpha(\gamma_f \mathbf{u}) \mathbf{g}_\tau \Big),$$

where ∇_τ denote the tangential gradient operator, and $\mathbf{g}$ the gravity vector, $\mathbf{g}_\tau = \mathbf{g} - (\mathbf{g}\cdot\mathbf{n})\mathbf{n}$) and $\mathbf{n}$ the unit normal vector to the fracture. At fracture intersections Σ, for $\alpha = g, l$, it is assumed that the pressures $\gamma_f p^\alpha$ are continuous and that the normal fluxes of the Darcy velocities $\mathbf{V}_f^\alpha$ sum to zero. At the immersed fracture boundary, the normal flux of the Darcy velocity $\mathbf{V}_f^\alpha$ is also assumed to vanish.

In the matrix domain, the Darcy velocities are classicaly defined by

$$\mathbf{V}_m^\alpha = -\frac{k_{r,m}^\alpha(\mathbf{x}, s_m^\alpha(p^g - p^l))}{\mu^\alpha(\mathbf{u})} \mathbf{K}_m(\mathbf{x}) \Big(\nabla p^\alpha - \rho^\alpha(\mathbf{u}) \mathbf{g} \Big),$$

for both phases $\alpha = g, l$.

In the gallery, the primary unknowns, depending only on the x coordinate along the gallery and on the time t, are the gas pressure p and the gas molar fractions $c = (c_e, c_a)$. The gas flow model is defined by a No Pressure Wave (NPW) [14] isothermal pipe flow model. To fix ideas a Forccheimer law is used for the pressure drop given by the two parameters $\alpha > 0$, $\beta > 0$ such that the velocity in the gallery is given by

$$w = h(\partial_x p) = \frac{\alpha - \sqrt{\alpha^2 + 4\beta|\partial_x p|}}{2\beta} \frac{\partial_x p}{|\partial_x p|}.$$

At the interface Γ between the gallery and the porous medium the coupling conditions are an adaptation to a 1D configuration for the free flow to those stated in [13]. Compared with [13], the gas pressure jump $p - p^g$ at the interface is neglected since a small flow rate between the porous medium and the gallery is assumed due to the low permeability of the disposal. Hence the coupling conditions account first for the continuity of the gas phase pressure $p^g = p$. Second, as in [13], we impose the continuity of the gas molar fractions $c^g = c$. Third the thermodynamical equilibrium between the gas phase and the liquid phase at the interface Γ is assumed. All together, we obtain the following coupling conditions at the interface Γ

$$\left\{ \begin{array}{l} p = p^g, \\ c_i = c_i^g(p^g, p^l), i = e, a. \end{array} \right. \tag{1}$$

Using these coupling conditions (1), we can formulate the 1D free flow model in the gallery as the following set of Ventcell type boundary conditions for $\mathbf{u}$ at the interface Γ

$$\left\{ \begin{array}{r} \partial_t\Big(|S|\zeta^g(\gamma\mathbf{u})c_i^g(\gamma\mathbf{u})\Big) + \partial_x\Big(|S|\zeta^g(\gamma\mathbf{u})c_i^g(\gamma\mathbf{u})h(\partial_x\gamma p^g)\Big) = Q_i, \\ \partial_s\mathbf{u} = 0, \end{array} \right. \tag{2}$$

$i = e, a$, where Q_i is a source term involving gas and liquid Darcy matrix and fracture fluxes on respectively Γ and $\Gamma \cap \partial\Gamma_f$ summed over both phases $\alpha = g, l$ assuming an instantaneous vaporization of the liquid phase in the gallery. These source terms can be recovered from the weak formulation (3).

For $\alpha = g, l$, $i = e, a$, let us denote the number of mole per unit matrix volume by

$$n_{i,m}^\alpha(\mathbf{x}, \mathbf{u}) = \phi_m(\mathbf{x})\zeta^\alpha(\mathbf{u})s_m^\alpha(\mathbf{x}, p^g - p^l)c_i^\alpha(\mathbf{u})$$

and the number of mole per unit fracture surface by

$$n_{i,f}^\alpha(\mathbf{x}, \gamma_f\mathbf{u}) = \phi_f(\mathbf{x})d_f(\mathbf{x})\zeta^\alpha(\gamma_f\mathbf{u})s_f^\alpha(\mathbf{x}, \gamma_f(p^g - p^l))c_i^\alpha(\gamma_f\mathbf{u}).$$

For $\alpha = g, l$, $i = e, a$, let us denote the mobility of the component i in phase α by

$$m_{i,m}^\alpha(\mathbf{x}, \mathbf{u}) = \zeta^\alpha(\mathbf{u})c_i^\alpha(\mathbf{u})\frac{k_{r,m}^\alpha(\mathbf{x}, s_m^\alpha(\mathbf{x}, p^g - p^l))}{\mu^\alpha(\mathbf{u})}$$

in the matrix, and by

$$m_{i,f}^\alpha(\mathbf{x}, \gamma_f\mathbf{u}) = \zeta^\alpha(\gamma_f\mathbf{u})c_i^\alpha(\gamma_f\mathbf{u})\frac{k_{r,f}^\alpha(\mathbf{x}, s_f^\alpha(\mathbf{x}, \gamma_f(p^g - p^l)))}{\mu^\alpha(\gamma_f\mathbf{u})}$$

in the fracture network.

We can now state the variational formulation of our model coupling the 3D gas liquid Darcy flow in the matrix domain, the 2D gas liquid Darcy flow in the fracture network, and the 1D free gas flow in the gallery.

Let $\mathcal{C}$ be the space of $C^\infty(\overline{\Omega}\times[0,T_f])$ functions vanishing in a neighbourhood of $\partial\Omega\backslash\Gamma\times[0,T_f]$ and of $\overline{\Omega}\times\{T_f\}$, and depending only on (x,t) in a neighbourhood of $\overline{\Gamma}\times[0,T_f]$.

Let be given physically admissible initial conditions $\mathbf{u}_{ini}$ on Ω, and p_{ini}, $c_{e,ini}\geq 0$, $c_{a,ini}=1-c_{e,ini}\geq 0$ on $(0,L)$, and physically admissible Dirichlet boundary conditions $\bar{\mathbf{u}}$ on $\Gamma_D=\partial\Omega\setminus\overline{\Gamma}$, and $\bar{\mathbf{u}}_0\in\mathbb{R}^2$, $\bar{\mathbf{u}}_L\in\mathbb{R}^2$ at both ends of $(0,L)$.

Formally, the variational formulation looks for $\mathbf{u}$ on $\Omega\times(0,T_f)$ satisfying $\partial_s\gamma\mathbf{u}=0$ on $\Gamma\times(0,T_f)$, the Dirichlet boundary conditions $\mathbf{u}=\bar{\mathbf{u}}$ on Γ_D, $\gamma_f\mathbf{u}=\gamma_f\bar{\mathbf{u}}$ on Σ_0, $\gamma\mathbf{u}(x=0,t)=\bar{\mathbf{u}}_0$, $\gamma\mathbf{u}(x=L,t)=\bar{\mathbf{u}}_L$, and such that for all $(v_e,v_a)\in\mathcal{C}^2$ and for $i=e,a$ one has:

$$
\begin{aligned}
&\sum_{\alpha=g,l}\Big(-\int_0^{T_f}\int_\Omega n_{i,m}^\alpha(\mathbf{x},\mathbf{u})\ \partial_t v_i\ d\mathbf{x}dt-\int_\Omega n_{i,m}^\alpha(\mathbf{x},\mathbf{u}_{ini})\ v_i(\mathbf{x},0)\ d\mathbf{x}\Big)\\
&+\sum_{\alpha=g,l}\int_0^{T_f}\int_\Omega m_{i,m}^\alpha(\mathbf{x},\mathbf{u})\mathbf{K}_m\Big(\nabla p^\alpha-\rho^\alpha(\mathbf{u})\mathbf{g}\Big)\cdot\nabla v_i\ d\mathbf{x}dt\\
&-\sum_{\alpha=g,l}\int_0^{T_f}\int_{\Gamma_f} n_{i,f}^\alpha(\mathbf{x},\gamma_f\mathbf{u})\ \partial_t\gamma_f v_i\ d\tau(\mathbf{x})dt\\
&-\sum_{\alpha=g,l}\int_{\Gamma_f} n_{i,f}^\alpha(\mathbf{x},\gamma_f\mathbf{u}_{ini})\ \gamma_f v_i(\mathbf{x},0)\ d\tau(\mathbf{x})\\
&+\sum_{\alpha=g,l}\int_0^{T_f}\int_{\Gamma_f} m_{i,f}^\alpha(\mathbf{x},\gamma_f\mathbf{u})d_f\mathbf{K}_f\Big(\nabla_\tau\gamma_f p^\alpha-\rho^\alpha(\gamma_f\mathbf{u})\mathbf{g}_\tau\Big)\cdot\nabla_\tau\gamma_f v_i\ d\tau(\mathbf{x})dt\\
&-\int_0^{T_f}|S|\int_0^L\zeta^g(\gamma\mathbf{u})c_i^g(\gamma\mathbf{u})\ \partial_t\gamma v_i\ dxdt-|S|\int_0^L\zeta^g(p_{ini})c_{i,ini}\gamma v_i\ dx\\
&+\int_0^{T_f}|S|\int_0^L\zeta^g(\gamma\mathbf{u})c_i^g(\gamma\mathbf{u})h(\partial_x\gamma p^g)\ \partial_x\gamma v_i\ dxdt=0.
\end{aligned}
\tag{3}
$$

3 Vertex Approximate Gradient discretization

In order to introduce the VAG discretization of our model let us first consider the coupling of a single phase Darcy flow in the fractured porous medium with a 1D single phase Darcy flow in the gallery. The discretization of the VAG fluxes and control volumes will be derived from this simple model and then used for the discretization of the previous full model.

3.1 Linear Model Problem

The space $H^1(\Gamma_f)\subset L^2(\Gamma_f)$ is defined as the subspace of functions with restriction to Γ_{f_i} in $H^1(\Gamma_{f_i})$, $i\in I$, and with continuous trace at fracture intersections. Our variational space is defined as follows

$$V=\{u\in H^1(\Omega)\,|\,\gamma_f u\in H^1(\Gamma_f),\,\gamma u\in H^1(\Gamma),\partial_s\gamma u=0\}.$$

Keeping the same notation for conveniency, the trace operator γ maps V to $H^1(0,L)$. The subspace of V taking into account homogeneous Dirichlet boundary conditions for u on Γ_D, for $\gamma_f u$ on Σ_0, and for γu at $x=0$ and $x=L$, is denoted by

$$V^0=\{u\in V\,|\,u=0\text{ on }\Gamma_D,\,\gamma_f u=0\text{ on }\Sigma_0,\,\gamma u(0)=\gamma u(L)=0\},$$

and endowed with the Hilbertian norm

$$\|u\|_{V^0} = \Big(\int_\Omega |\nabla u(\mathbf{x})|^2 d\mathbf{x} + \int_{\Gamma_f} |\nabla_\tau \gamma_f u(\mathbf{x})|^2 d\tau(\mathbf{x}) + \int_0^L |\frac{d}{dx}\gamma u(x)|^2 dx\Big)^{\frac{1}{2}}.$$

Let $h_m \in L^2(\Omega)$, $h_f \in L^2(\Gamma_f)$, and $h_g \in L^2(0,L)$ denote respectively the source terms in the matrix, in the fracture network, and in the gallery. Let $\bar{u} \in V$, and let us consider the linear model coupling a single phase Darcy flow in the fractured porous medium with a single phase Darcy flow in the gallery. Its variational formulation amounts to find $u \in V$ such that $u - \bar{u} \in V^0$ and

$$\begin{aligned} &\int_\Omega \mathbf{K}_m \nabla u \cdot \nabla v \; d\mathbf{x} + \int_\Omega d_f \mathbf{K}_f \nabla_\tau \gamma_f u \cdot \nabla_\tau \gamma_f v \; d\tau(\mathbf{x}) \\ &\qquad + \int_0^L \frac{|S|}{\alpha} \partial_x \gamma u \partial_x \gamma v \; dx \\ &= \int_\Omega h_m v \; d\mathbf{x} + \int_{\Gamma_f} d_f h_f \; \gamma_f v \; d\tau(\mathbf{x}) + \int_0^L |S| h_g \gamma v \; dx. \end{aligned} \tag{4}$$

for all $v \in V^0$. The existence and uniqueness of a solution to (4) is readily obtained from the Poincaré inequality and the Lax Milgram theorem.

3.2 VAG Discretization of the Linear Model Problem

The VAG discretization [10] is a finite volume discretization of diffusion problem adapted to general meshes and heterogenous anisotropic media. It is here extended to our model problem coupling the 3D Darcy flow in the porous medium, the 2D Darcy flow in the fracture network and the 1D Darcy flow in the gallery.

We assume that ω and S are polygonal domains of $\mathbb{R}^2$ and we consider a conforming polyhedral mesh of the domain Ω. Let $\mathcal{M}$ denote the set of cells K, $\mathcal{V}$ the set of vertices $\mathbf{s}$, $\mathcal{E}$ the set of edges e, and $\mathcal{F}$ the set of faces σ, of the mesh. We denote by $\mathcal{V}_K$ the set of vertices of each cell $K \in \mathcal{M}$, by $\mathcal{M}_s$ the set of cells sharing the node s, by $\mathcal{V}_\sigma$ the set of nodes and by $\mathcal{E}_\sigma$ the set of edges of the face $\sigma \in \mathcal{F}$. The set $\mathcal{M}_\sigma$ is the set of cells shared by the face $\sigma \in \mathcal{F}$. We denote by $\mathcal{V}_\Gamma = \mathcal{V} \cap \overline{\Gamma}$ the set of nodes belonging to the boundary Γ of the gallery, and by $\mathcal{V}_D = \mathcal{V} \cap \Gamma_D$ the set of Dirichlet boundary nodes. In the following, for a d dimensional domain A, $|A|$ will denote the Lebesgue d-dimensional measure of A.

It is assumed that for each face $\sigma \in \mathcal{F}$, there exists a so-called "centre" of the face $\mathbf{x}_\sigma$ such that $\mathbf{x}_\sigma = \frac{1}{\mathrm{Card}(\mathcal{V}_\sigma)} \sum_{\mathbf{s} \in \mathcal{V}_\sigma} \mathbf{x}_\mathbf{s}$. The face σ is assumed to be star-shaped w.r.t. its centre $\mathbf{x}_\sigma$ which means that the face σ matches with the union of the triangles $\tau_{\sigma,e}$ defined by the face centre $\mathbf{x}_\sigma$ and each of its edge $e \in \mathcal{E}_\sigma$.

The porous medium mesh is assumed to be conforming with respect to the fracture network in the sense that there exists $\mathcal{F}_{\Gamma_f} \subset \mathcal{F}$ such that

$$\overline{\Gamma}_f = \bigcup_{\sigma \in \mathcal{F}_{\Gamma_f}} \overline{\sigma}.$$

Let us denote by $\mathcal{F}_{\Gamma_f,\mathbf{s}}$ the set of fracture faces sharing the node $\mathbf{s} \in \mathcal{V}_{\Gamma_f} = \mathcal{V} \cap \overline{\Gamma}_f$.

A finite element 1D mesh is defined in the gallery $(0,L)$ by the set of nodal points $0 = x_0 < \cdots < x_m < x_{m+1} < \cdots < x_{m_x+1} = L$. The $\mathbb{P}_1$ finite element nodal basis defined on this 1D mesh

is denoted by η_m, $m = 0, \cdots, m_x + 1$. Setting $x_{m+\frac{1}{2}} = \frac{x_m + x_{m+1}}{2}$ for all $m = 1, \cdots, m_x - 1$, and $x_{\frac{1}{2}} = 0$, $x_{m_x+\frac{1}{2}} = L$, we define the m_x 1D cells $k_m = (x_{m-\frac{1}{2}}, x_{m+\frac{1}{2}})$ and 3D cells $K_m = k_m \times S$, $m = 1, \cdots, m_x$.

The previous discretization is denoted by $\mathcal{D}$. Let us define the vector space

$$X_{\mathcal{D}_p} = \{v_K \in \mathbb{R}, v_{\mathbf{s}} \in \mathbb{R}, v_\sigma \in \mathbb{R},\ K \in \mathcal{M}, \mathbf{s} \in \mathcal{V}, \sigma \in \mathcal{F}_{\Gamma_f}\},$$

of degrees of freedom (d.o.f.) located at the cell centres, fracture face centres, and at the nodes of the porous medium mesh, and the vector space

$$X_{\mathcal{D}_g} = \{v_m \in \mathbb{R}, m = 0, \cdots, m_x + 1\},$$

of d.o.f. located at the nodal points of the gallery $(0, L)$.

The extension of the VAG discretization [10] to our coupled model is based on conforming Finite Element reconstructions of the gradient operators on Ω, on Γ_f, and on $(0, L)$, and on non conforming piecewise constant function reconstructions on Ω, on Γ_f, and on $(0, L)$.

For all $\sigma \in \mathcal{F}$, let us first define the operator $I_\sigma : X_{\mathcal{D}_p} \to \mathbb{R}$ such that $I_\sigma(v_\mathcal{D}) = \frac{1}{\mathrm{Card}(\mathcal{V}_\sigma)} \sum_{\mathbf{s} \in \mathcal{V}_\sigma} v_{\mathbf{s}}$, which is by definition of $\mathbf{x}_\sigma$ a second order interpolation operator at point $\mathbf{x}_\sigma$.

Let us introduce the tetrahedral sub-mesh $\mathcal{T} = \{T_{K,\sigma,e}, e \in \mathcal{E}_\sigma, \sigma \in \mathcal{F}_K, K \in \mathcal{M}\}$ of the porous medium mesh, where $T_{K,\sigma,e}$ is the tetrahedron defined by the cell center $\mathbf{x}_K$ and the triangle $\tau_{\sigma,e}$. For a given $v_{\mathcal{D}_p} \in X_{\mathcal{D}_p}$, we define the function $\Pi_\mathcal{T} v_{\mathcal{D}_p} \in C^0(\overline{\Omega})$ as the continuous piecewise affine function on each tetrahedron of $\mathcal{T}$ such that $\Pi_\mathcal{T} v_{\mathcal{D}_p}(\mathbf{x}_K) = v_K$, $\Pi_\mathcal{T} v_{\mathcal{D}_p}(\mathbf{s}) = v_{\mathbf{s}}$, $\Pi_\mathcal{T} v_{\mathcal{D}_p}(\mathbf{x}_\sigma) = v_\sigma$, and $\Pi_\mathcal{T} v_{\mathcal{D}_p}(\mathbf{x}_{\sigma'}) = I_{\sigma'}(v)$ for all $K \in \mathcal{M}$, $\mathbf{s} \in \mathcal{V}$, $\sigma \in \mathcal{F}_{\Gamma_f}$, and $\sigma' \in \mathcal{F} \setminus \mathcal{F}_{\Gamma_f}$.

The nodal finite element basis of $\Pi_\mathcal{T} X_{\mathcal{D}_p}$ is denoted by η_ν, $\nu \in \mathcal{M} \cup \mathcal{V} \cup \mathcal{F}_{\Gamma_f}$ such that $\eta_\nu(\mathbf{x}_{\nu'}) = \delta_{\nu,\nu'}$ for all $\nu, \nu' \in \mathcal{M} \cup \mathcal{V} \cup \mathcal{F}_{\Gamma_f}$.

Then, we define for all $v_{\mathcal{D}_p} \in X_{\mathcal{D}_p}$ the following gradient operators

$$\nabla_{\mathcal{D}_m} v_{\mathcal{D}_p} : X_{\mathcal{D}_p} \to L^2(\Omega)^d \text{ such that } \nabla_{\mathcal{D}_m} v_{\mathcal{D}_p} = \nabla \Pi_\mathcal{T} v_{\mathcal{D}_p},$$

in the matrix, and

$$\nabla_{\mathcal{D}_f} v_{\mathcal{D}_p} : X_{\mathcal{D}_p} \to L^2(\Gamma_f)^{d-1} \text{ such that } \nabla_{\mathcal{D}_f} v_{\mathcal{D}_p} = \nabla_\tau \gamma_f \Pi_\mathcal{T} v_{\mathcal{D}_p}.$$

in the fracture network. In the gallery, the gradient operator $\nabla_{\mathcal{D}_g}$ from $X_{\mathcal{D}_g}$ to $L^2(0, L)$ is defined by

$$\nabla_{\mathcal{D}_g} v_{\mathcal{D}_g}(x) = \frac{v_{m+1} - v_m}{x_{m+1} - x_m} \text{ for all } x \in (x_m, x_{m+1}), m = 0, \cdots, m_x.$$

In addition to these conforming gradient operators, the VAG discretization uses non conforming piecewise constant reconstructions of functions from $X_{\mathcal{D}_p}$ into $L^2(\Omega)$ abd $L^2(\Gamma_f)$, and from $X_{\mathcal{D}_g}$ into $L^2(0, L)$.

Let us introduce the following partition of each cell $K \in \mathcal{M}$

$$\overline{K} \ = \ \overline{\omega}_K \bigcup \Big(\bigcup_{\mathbf{s} \in \mathcal{V}_K \setminus (\mathcal{V}_D \cup \mathcal{V}_\Gamma \cup \mathcal{V}_{\Gamma_f})} \overline{\omega}_{K,\mathbf{s}} \Big)$$

Then, we define the function reconstruction operator in the matrix

$$\Pi_{\mathcal{D}_m} v_{\mathcal{D}_p}(\mathbf{x}) = \begin{cases} v_K & \text{for all } \mathbf{x} \in \omega_K,\ K \in \mathcal{M}, \\ v_{\mathbf{s}} & \text{for all } \mathbf{x} \in \omega_{K,\mathbf{s}},\ \mathbf{s} \in \mathcal{V}_K \setminus (\mathcal{V}_D \cup \mathcal{V}_\Gamma \cup \mathcal{V}_{\Gamma_f}),\ K \in \mathcal{M}. \end{cases} \tag{5}$$

Similarly, let us define the partition of each fracture face $\sigma \in \mathcal{F}_{\Gamma_f}$ by

$$\overline{\sigma} \;=\; \overline{\Sigma}_\sigma \bigcup \Big(\bigcup_{\mathbf{s}\in\mathcal{V}_\sigma\setminus(\mathcal{V}_D\cup\mathcal{V}_\Gamma)} \overline{\Sigma}_{\sigma,\mathbf{s}}\Big),$$

and the function reconstruction operator in the fracture network by

$$\Pi_{\mathcal{D}_f} v_{\mathcal{D}_p}(\mathbf{x}) = \left\{ \begin{array}{ll} v_\sigma & \text{for all } \mathbf{x}\in\Sigma_\sigma,\ \sigma\in\mathcal{F}_{\Gamma_f}, \\ v_\mathbf{s} & \text{for all } \mathbf{x}\in\Sigma_{\sigma,\mathbf{s}},\ \mathbf{s}\in\mathcal{V}_\sigma\setminus(\mathcal{V}_D\cup\mathcal{V}_\Gamma),\ \sigma\in\mathcal{F}_{\Gamma_f}. \end{array}\right. \tag{6}$$

In the gallery, the reconstruction operator is defined by

$$\Pi_{\mathcal{D}_g} v_\mathcal{D}(x) = v_m \text{ for all } x\in(x_{m-\frac{1}{2}}, x_{m+\frac{1}{2}}),\ m=1,\cdots,m_x. \tag{7}$$

Finally, let us define the interpolation operator $\mathcal{P}_\mathbf{s}$ reconstructing the value $u_\mathbf{s}$ at point $\mathbf{x}_\mathbf{s}$ for $\mathbf{s}\in\mathcal{V}_\Gamma$ as a function of the vector of d.o.f. $u_{\mathcal{D}_g}\in X_{\mathcal{D}_g}$ in the gallery:

$$\mathcal{P}_\mathbf{s} u_{\mathcal{D}_g} = \sum_{m=0}^{m_x+1} \alpha_{m,\mathbf{s}} u_m,$$

with $\alpha_{m,\mathbf{s}} = \eta_m(x_\mathbf{s})$. From this definition of $\mathcal{P}_\mathbf{s}$, we can define the vector space $X_\mathcal{D}$ of discrete unknowns as the following subspace of $X_{\mathcal{D}_p}\times X_{\mathcal{D}_g}$

$$X_\mathcal{D} = \{(v_{\mathcal{D}_p}, v_{\mathcal{D}_g})\in X_{\mathcal{D}_p}\times X_{\mathcal{D}_g} \,|\, v_\mathbf{s} = \mathcal{P}_s v_{\mathcal{D}_g} \text{ for all } \mathbf{s}\in\mathcal{V}_\Gamma\}.$$

Its subspace with homogeneous Dirichlet boundary conditions is denoted by

$$X_\mathcal{D}^0 = \{v_\mathcal{D}\in X_\mathcal{D} \,|\, v_\mathbf{s} = 0 \text{ for all } \mathbf{s}\in\mathcal{V}_D, \text{ and } v_0 = v_{m_x+1} = 0\}.$$

The previous gradient and function reconstruction operators will be applied on vectors of $X_\mathcal{D}$ keeping the same notations for convenience sake.

The VAG discretization of our model problem is obtained by the following non conforming variational formulation: given $\bar{u}_\mathcal{D}\in X_\mathcal{D}$, find $u_\mathcal{D}\in X_\mathcal{D}$ such that $u_\mathcal{D}-\bar{u}_\mathcal{D}\in X_\mathcal{D}^0$ and

$$\begin{aligned} &\int_\Omega \mathbf{K}_m \nabla_{\mathcal{D}_m} u_\mathcal{D}\cdot\nabla_{\mathcal{D}_m} v_\mathcal{D}\ d\mathbf{x} + \int_{\Gamma_f} d_f \mathbf{K}_f \nabla_{\mathcal{D}_f} u_\mathcal{D}\cdot\nabla_{\mathcal{D}_f} v_\mathcal{D}\ d\tau(\mathbf{x}) \\ &+ \int_0^L \frac{|S|}{\alpha}\nabla_{\mathcal{D}_g} u_\mathcal{D}\nabla_{\mathcal{D}_g} v_\mathcal{D}\ dx \\ &= \int_\Omega h_m \Pi_{\mathcal{D}_m} v_\mathcal{D}\ d\mathbf{x} + \int_{\Gamma_f} d_f h_f \Pi_{\mathcal{D}_f} v_\mathcal{D}\ d\tau(\mathbf{x}) + \int_0^L |S| h_g \Pi_{\mathcal{D}_g} v_\mathcal{D}\ dx, \end{aligned} \tag{8}$$

for all $v_\mathcal{D}\in X_\mathcal{D}^0$.

In order to write the equivalent finite volume formulation of (8), let us define for all $u_\mathcal{D}\in X_\mathcal{D}$ the matrix fluxes

$$V_{K,\nu}(u_\mathcal{D}) = \sum_{\nu'\in\Xi_K} T_K^{\nu,\nu'}(u_K - u_{\nu'}), \tag{9}$$

connecting each cell K to its d.o.f. $\nu\in\Xi_K$ with $\Xi_K = \mathcal{V}_K\cup(\mathcal{F}_K\cap\mathcal{F}_{\Gamma_f})$ and

$$T_K^{\nu,\nu'} = \int_K \mathbf{K}_m\nabla\eta_\nu\cdot\nabla\eta_{\nu'} d\mathbf{x}.$$

Similarly, the fracture fluxes defined by

$$V_{\sigma,\mathbf{s}}(u_{\mathcal{D}}) = \sum_{\nu' \in \mathcal{V}_\sigma} T_\sigma^{\mathbf{s},\mathbf{s}'}(u_\sigma - u_{\mathbf{s}'}), \tag{10}$$

connect each fracture face σ to its nodes $\mathbf{s} \in \mathcal{V}_\sigma$ where

$$T_\sigma^{\mathbf{s},\mathbf{s}'} = \int_\sigma d_f \mathbf{K}_f \nabla_\tau \gamma_f \eta_{\mathbf{s}} \cdot \nabla_\tau \gamma_f \eta_{\mathbf{s}'} d\tau(\mathbf{x}).$$

On the gallery side, we similarly define for all $u_{\mathcal{D}} \in X_{\mathcal{D}}$ the fluxes

$$V_{m,m+1}(u_{\mathcal{D}}) = T_{m+\frac{1}{2}}(u_m - u_{m+1}), \tag{11}$$

connecting m to $m+1$ for all $m = 0, \cdots, m_x$, where

$$T_{m+\frac{1}{2}} = \frac{|S|}{(x_{m+1} - x_m)^2} \int_{x_m}^{x_{m+1}} \frac{dx}{\alpha(x)}.$$

Let us set for the source terms in the matrix

$$h_{m,K} = \frac{1}{|\omega_K|} \int_{\omega_K} h_m(\mathbf{x}) d\mathbf{x}, \quad h_{m,K,\mathbf{s}} = \frac{1}{|\omega_{K,\mathbf{s}}|} \int_{\omega_{K,\mathbf{s}}} h_m(\mathbf{x}) d\mathbf{x},$$

and $\alpha_{K,\mathbf{s}} = \frac{|\omega_{K,\mathbf{s}}|}{|K|}$ for all $\mathbf{s} \in \mathcal{V}_K \setminus (\mathcal{V}_D \cup \mathcal{V}_\Gamma \cup \mathcal{V}_{\Gamma_f})$ and $K \in \mathcal{M}$. Similarly, we set in the fracture network

$$h_{f,\sigma} = \frac{1}{|\Sigma_\sigma|} \int_{\Sigma_\sigma} d_f(\mathbf{x}) h_f(\mathbf{x}) d\tau(\mathbf{x}), \quad h_{f,\sigma,\mathbf{s}} = \frac{1}{|\Sigma_{\sigma,\mathbf{s}}|} \int_{\Sigma_{\sigma,\mathbf{s}}} d_f(\mathbf{x}) h_f(\mathbf{x}) d\tau(\mathbf{x}),$$

and $\alpha_{\sigma,\mathbf{s}} = \frac{|\Sigma_{\sigma,\mathbf{s}}|}{|\sigma|}$ for all $\mathbf{s} \in \mathcal{V}_\sigma \setminus (\mathcal{V}_D \cup \mathcal{V}_\Gamma)$ and $\sigma \in \mathcal{F}_{\Gamma_f}$.

Then, the variational formulation (8) is equivalent to find $u_{\mathcal{D}} \in X_{\mathcal{D}}$ satisfying the discrete conservation equations in the porous medium

$$\begin{cases} \displaystyle\sum_{\nu \in \Xi_K} V_{K,\nu}(u_{\mathcal{D}}) = (1 - \sum_{\mathbf{s} \in \mathcal{V}_K \setminus (\mathcal{V}_D \cup \mathcal{V}_\Gamma \cup \mathcal{V}_{\Gamma_f})} \alpha_{K,\mathbf{s}}) |K| h_{m,K},\ K \in \mathcal{M}, \\ \displaystyle\sum_{\mathbf{s} \in \mathcal{V}_\sigma} V_{\sigma,\mathbf{s}}(u_{\mathcal{D}}) - \sum_{K \in \mathcal{M}_\sigma} V_{K,\sigma}(u_{\mathcal{D}}) = (1 - \sum_{\mathbf{s} \in \mathcal{V}_\sigma \setminus (\mathcal{V}_D \cup \mathcal{V}_\Gamma)} \alpha_{\sigma,\mathbf{s}}) |\sigma| h_{f,\sigma},\ \sigma \in \mathcal{F}_{\Gamma_f}, \\ \displaystyle -\sum_{K \in \mathcal{M}_{\mathbf{s}}} V_{K,\mathbf{s}}(u_{\mathcal{D}}) = \sum_{K \in \mathcal{M}_{\mathbf{s}}} \alpha_{K,\mathbf{s}} |K| h_{m,K,\mathbf{s}},\ \mathbf{s} \in \mathcal{V} \setminus (\mathcal{V}_D \cup \mathcal{V}_\Gamma \cup \mathcal{V}_{\Gamma_f}), \\ \displaystyle -\sum_{K \in \mathcal{M}_{\mathbf{s}}} V_{K,\mathbf{s}}(u_{\mathcal{D}}) - \sum_{\sigma \in \mathcal{F}_{\Gamma_f,\mathbf{s}}} V_{\sigma,\mathbf{s}}(u_{\mathcal{D}}) \\ \qquad \displaystyle = \sum_{\sigma \in \mathcal{F}_{\Gamma_f,\mathbf{s}}} \alpha_{\sigma,\mathbf{s}} |\sigma| h_{f,\sigma,\mathbf{s}},\ \mathbf{s} \in \mathcal{V}_{\Gamma_f} \setminus (\mathcal{V}_D \cup \mathcal{V}_\Gamma), \\ u_{\mathbf{s}} = \bar{u}_{\mathbf{s}},\ \mathbf{s} \in \mathcal{V}_D, \end{cases} \tag{12}$$

coupled with the conservation equations in the gallery for $m = 1, \cdots, m_x$

$$\begin{aligned} V_{m,m+1}(u_{\mathcal{D}}) - V_{m-1,m}(u_{\mathcal{D}}) &= \int_{x_{m-1/2}}^{x_{m+1/2}} |S| h_g \, dx \\ &+ \sum_{\mathbf{s} \in \mathcal{V}_\Gamma} \alpha_{m,\mathbf{s}} \Big(\sum_{K \in \mathcal{M}_{\mathbf{s}}} V_{K,\mathbf{s}}(u_{\mathcal{D}}) + \sum_{\sigma \in \mathcal{F}_{\Gamma_f,\mathbf{s}}} V_{\sigma,\mathbf{s}}(u_{\mathcal{D}}) \Big), \end{aligned} \tag{13}$$

and the boundary conditions at the end points of the gallery $u_0 = \bar{u}_0$, $u_{m_x+1} = \bar{u}_{m_x+1}$. Note that the right hand side h_m does not appear in the conservation equations in the fracture network, and that the right hand sides h_m and h_f do not appear in the conservation equations in the gallery. This is due to our choice of the operators $\Pi_{\mathcal{D}_m}$ and $\Pi_{\mathcal{D}_f}$ which avoid the mixing of the matrix and fractures in the control volumes located at nodes $\mathbf{s} \in \mathcal{V}_{\Gamma_f}$, as well as the mixing of the porous medium and the gallery in control volumes located at nodes $\mathbf{s} \in \mathcal{V}_\Gamma$. This is a crutial property to extend the VAG discretization to the compositional model taking into account the highly contrasted material properties or the different models in the gallery, in the fractures, and in the matrix.

3.3 Extension to the Compositional Model

The VAG scheme has been extended to multiphase Darcy flows in [8] for compositional models. In [9] it is adapted to the case of discontinuous capillary pressures using a phase pressure formulation in order to take into account accurately the saturation jump at the interfaces between different rocktypes. This motivates the choice of the phase pressures as primary unknowns in our model. In [5] it is extended to the case of immiscible two phase Darcy flows in discrete fracture networks coupling the flow in the fractures with the flow in the surrounding matrix. The current discretization combines ideas of [9] and [5] and extend them to compositional models and to the coupling with the 1D free gas flow.

Let us define $\mathbf{u}_\mathcal{D} = (p^g_\mathcal{D}, p^l_\mathcal{D}) \in (X_\mathcal{D})^2$ as the vector of the discrete unknowns of the coupled model (3). The discretization of the Darcy matrix fluxes for each component $i = e, a$ combines the VAG fluxes and a phase by phase upwinding of the mobility terms w.r.t. the sign of the flux

$$V^\alpha_{K,\nu,i}(\mathbf{u}_\mathcal{D}) = m^\alpha_{i,m}(\mathbf{x}_K, \mathbf{u}^{\alpha,up}_{K,\nu})\Big(V_{K,\nu}(p^\alpha_\mathcal{D}) + g\rho^\alpha_{K,\nu}V_{K,\nu}(z_\mathcal{D})\Big),$$

for all $K \in \mathcal{M}$, $\nu \in \Xi_K$, with the upwinding

$$\mathbf{u}^{\alpha,up}_{K,\nu} = \begin{cases} \mathbf{u}_K & \text{if} \quad V_{K,\nu}(p^\alpha_\mathcal{D}) + g\rho^\alpha_{K,\nu}V_{K,\nu}(z_\mathcal{D}) \geq 0, \\ \mathbf{u}_\nu & \text{else}, \end{cases}$$

the averaged density $\rho^\alpha_{K,\nu} = \frac{\rho^\alpha(\mathbf{u}_K)+\rho^\alpha(\mathbf{u}_\nu)}{2}$, and the vector of the vertical coordinates at all d.o.f. $z_\mathcal{D} = (z_\mu, \mu \in \mathcal{M} \cup \mathcal{V} \cup \mathcal{F}_{\Gamma_f})$.

Similarly, the discretization of the Darcy fracture fluxes for $\sigma \in \mathcal{F}_{\Gamma_f}$, $\mathbf{s} \in \mathcal{V}_\sigma$ is defined by

$$V^\alpha_{\sigma,\mathbf{s},i}(\mathbf{u}_\mathcal{D}) = m^\alpha_{i,f}(\mathbf{x}_\sigma, \mathbf{u}^{\alpha,up}_{\sigma,\mathbf{s}})\Big(V_{\sigma,\mathbf{s}}(p^\alpha_\mathcal{D}) + g\rho^\alpha_{\sigma,\mathbf{s}}V_{\sigma,\mathbf{s}}(z_\mathcal{D})\Big),$$

with the upwinding

$$\mathbf{u}^{\alpha,up}_{\sigma,\mathbf{s}} = \begin{cases} \mathbf{u}_\sigma & \text{if} \quad V_{\sigma,\mathbf{s}}(p^\alpha_\mathcal{D}) + g\rho^\alpha_{\sigma,\mathbf{s}}V_{\sigma,\mathbf{s}}(z_\mathcal{D}) \geq 0, \\ \mathbf{u}_\mathbf{s} & \text{else}, \end{cases}$$

and the averaged density $\rho^\alpha_{\sigma,\mathbf{s}} = \frac{\rho^\alpha(\mathbf{u}_\sigma)+\rho^\alpha(\mathbf{u}_\mathbf{s})}{2}$.

The VAG fluxes in the gallery (11) are extended to the Darcy-Forchheimer law using a one quadrature point formula as follows

$$\begin{aligned} V_{m,m+1}(p^g_\mathcal{D}) &= |S|h\left(\alpha(x_{m+\frac{1}{2}}), \beta(x_{m+\frac{1}{2}}), \nabla_{\mathcal{D}_g}p^g_\mathcal{D}(x_{m+\frac{1}{2}})\right) \\ &= |S|h\left(\alpha(x_{m+\frac{1}{2}}), \beta(x_{m+\frac{1}{2}}), \frac{p^g_{m+1} - p^g_m}{x_{m+1} - x_m}\right), \end{aligned}$$

and the discretization of the Darcy-Forchheimer fluxes for each component $i = e, a$ is defined by

$$V_{m,m+1,i}(\mathbf{u}_{\mathcal{D}}) = \zeta^g(\mathbf{u}^{up}_{m,m+1}) c_i^g(\mathbf{u}^{up}_{m,m+1}) V_{m,m+1}(p^g_{\mathcal{D}}),$$

with the upwinding

$$\mathbf{u}^{up}_{m,m+1} = \begin{cases} \mathbf{u}_m, & \text{if} \quad V_{m,m+1}(p^g_{\mathcal{D}}) \geq 0, \\ \mathbf{u}_{m+1}, & \text{else}, \end{cases}$$

for all $m = 0, \cdots, m_x$.

For $N \in \mathbb{N}^*$, let us consider the time discretization $t^0 = 0 < t^1 < \cdots < t^{n-1} < t^n \cdots < t^N = T_f$ of the time interval $[0, T_f]$. We denote the time steps by $\Delta t^n = t^n - t^{n-1}$ for all $n = 1, \cdots, N$.

The initial conditions are given in the porous medium by $\mathbf{u}^0_\nu = (p^g_{ini,\nu}, p^l_{ini,\nu})$ for all $\nu \in \mathcal{M} \cup \mathcal{F}_{\Gamma_f} \cup \Big(\mathcal{V} \backslash (\mathcal{V}_D \cup \mathcal{V}_\Gamma)\Big)$. In the gallery, they are defined for all $m = 1, \cdots, m_x$ by $p^{g,0}_m = p^g_{ini,m}$, and $p^{l,0}_m = p^l_{ini,m}$.

The system of discrete equations in the porous medium at time step t^n accounts for the discrete molar conservation of each component $i = e, a$ in each control volume $K \in \mathcal{M}$, $\sigma \in \mathcal{F}_{\Gamma_f}$, and $\mathbf{s} \in \mathcal{V} \setminus (\mathcal{V}_D \cup \mathcal{V}_\Gamma)$,

$$\begin{cases} \displaystyle\sum_{\alpha=g,l} (1 - \sum_{\mathbf{s} \in \mathcal{V}_K \backslash (\mathcal{V}_D \cup \mathcal{V}_\Gamma)} \alpha_{K,\mathbf{s}}) |K| \frac{n^\alpha_{i,m}(\mathbf{x}_K, \mathbf{u}^n_K) - n^\alpha_{i,m}(\mathbf{x}_K, \mathbf{u}^{n-1}_K)}{\Delta t^n} \\ \displaystyle + \sum_{\alpha=g,l} \sum_{\nu \in \Xi_K} V^\alpha_{K,\nu,i}(\mathbf{u}^n_{\mathcal{D}}) = 0, \; K \in \mathcal{M}, \\ \displaystyle\sum_{\alpha=g,l} (1 - \sum_{\mathbf{s} \in \mathcal{V}_\sigma \backslash (\mathcal{V}_D \cup \mathcal{V}_\Gamma)} \alpha_{\sigma,\mathbf{s}}) |\sigma| \frac{n^\alpha_{i,f}(\mathbf{x}_\sigma, \mathbf{u}^n_\sigma) - n^\alpha_{i,f}(\mathbf{x}_\sigma, \mathbf{u}^{n-1}_\sigma)}{\Delta t^n} \\ \displaystyle + \sum_{\alpha=g,l} \Big(\sum_{\mathbf{s} \in \mathcal{V}_\sigma} V^\alpha_{\sigma,\mathbf{s},i}(\mathbf{u}^n_{\mathcal{D}}) - \sum_{K \in \mathcal{M}_\sigma} V^\alpha_{K,\sigma,i}(\mathbf{u}^n_{\mathcal{D}}) \Big) = 0, \; \sigma \in \mathcal{F}_{\Gamma_f}, \\ \displaystyle\sum_{\alpha=g,l} \sum_{K \in \mathcal{M}_\mathbf{s}} \alpha_{K,\mathbf{s}} |K| \frac{n^\alpha_{i,m}(\mathbf{x}_K, \mathbf{u}^n_\mathbf{s}) - n^\alpha_{i,m}(\mathbf{x}_K, \mathbf{u}^{n-1}_\mathbf{s})}{\Delta t^n} \\ \displaystyle - \sum_{\alpha=g,l} \sum_{K \in \mathcal{M}_\mathbf{s}} V^\alpha_{K,\mathbf{s},i}(\mathbf{u}^n_{\mathcal{D}}) = 0, \; \mathbf{s} \in \mathcal{V} \setminus (\mathcal{V}_D \cup \mathcal{V}_\Gamma \cup \mathcal{V}_{\Gamma_f}), \\ \displaystyle \sum_{\sigma \in \mathcal{F}_{\Gamma_f,\mathbf{s}}} \alpha_{\sigma,\mathbf{s}} |\sigma| \frac{n^\alpha_{i,f}(\mathbf{x}_\sigma, \mathbf{u}^n_\mathbf{s}) - n^\alpha_{i,f}(\mathbf{x}_\sigma, \mathbf{u}^{n-1}_\mathbf{s})}{\Delta t^n} \\ \displaystyle - \sum_{\alpha=g,l} \Big(\sum_{K \in \mathcal{M}_\mathbf{s}} V^\alpha_{K,\mathbf{s},i}(\mathbf{u}^n_{\mathcal{D}}) + \sum_{\sigma \in \mathcal{F}_{\Gamma_f,\mathbf{s}}} V^\alpha_{\sigma,\mathbf{s},i}(\mathbf{u}^n_{\mathcal{D}}) \Big) = 0, \; \mathbf{s} \in \mathcal{V}_{\Gamma_f} \setminus (\mathcal{V}_D \cup \mathcal{V}_\Gamma), \end{cases}$$

together with the Dirichlet boundary conditions $\mathbf{u}^n_\mathbf{s} = (\bar{p}^g_\mathbf{s}, \bar{p}^l_\mathbf{s})$ for all $\mathbf{s} \in \mathcal{V}_D$. This system is coupled to the equations in the gallery at time step t^n accounting for the discrete molar conservation of each component $i = e, a$

$$\begin{aligned} & |K_m| \frac{\zeta^g(\mathbf{u}^n_m) c^g_i(\mathbf{u}^n_m) - \zeta^g(\mathbf{u}^{n-1}_m) c^g_i(\mathbf{u}^{n-1}_m)}{\Delta t^n} \\ & \qquad + V_{m,m+1,i}(\mathbf{u}^n_{\mathcal{D}}) - V_{m-1,m,i}(\mathbf{u}^n_{\mathcal{D}}) \\ & = \sum_{\mathbf{s} \in \mathcal{V}_\Gamma} \alpha_{m,\mathbf{s}} \sum_{\alpha=g,l} \Big(\sum_{K \in \mathcal{M}_\mathbf{s}} V^\alpha_{K,\mathbf{s},i}(\mathbf{u}^n_{\mathcal{D}}) + \sum_{\sigma \in \mathcal{F}_{\Gamma_f,\mathbf{s}}} V^\alpha_{\sigma,\mathbf{s},i}(\mathbf{u}^n_{\mathcal{D}}) \Big), \; m = 1, \cdots, m_x, \end{aligned}$$

and the Dirichlet conditions at both sides of the gallery $\mathbf{u}^n_0 = \bar{\mathbf{u}}_0$, $\mathbf{u}^n_{m_x+1} = \bar{\mathbf{u}}_L$.

4 Numerical tests

4.1 Test case with 1 fracture

Let ω and S be the disks of center 0 and radius respectively $r_\omega = 15$ m and $r_S = 2$ m. We consider a radial mesh of the domain $(0, L) \times (\omega \setminus \overline{S})$, $L = 100$ m of size $n_x = 40$, $n_r = 30$, $n_\theta = 32$ in the cylindrical coordinates x, r, θ. The porous medium includes a single fracture defined by $x = 50$ m, $\theta \in [0, 2\pi)$, $r \in (r_S, r_f)$ with $r_f = 10$ m. The mesh is uniform in the x and θ directions and is exponentially refined at the interface of the gallery Γ to account for the steep gradient of the capillary pressure at the porous medium gallery interface. The mesh in the gallery is conforming with the porous medium mesh in the sense that $m_x = n_x$ and that the points x_m, $m = 0, \cdots, m_x + 1$ match with the x coordinates of the nodes along the x direction in the porous medium.

The temperature is fixed at $T = 300$ K. The gas molar density is given by $\zeta^g(p^g) = \frac{p^g}{RT}$ mol.m^{-3} with $R = 8.314$ J K^{-1} mol^{-1}, and the liquid molar density is fixed to $\zeta^l = 55555$ mol.m^{-3}. The mass densities are related to the molar densities by $\rho^\alpha = \Big(\sum_{i=e,a} c_i^\alpha M_i\Big)\zeta^\alpha$, where M_i, $i = e, a$ are the molar masses of the components. Using the Henry law for the fugacity of the air component in the liquid phase, the Raoult-Kelvin's law for the fugacity of the water component in the liquid phase, and the Dalton's law for an ideal mixture of perfect gas for the fugacities of the air and water components in the gas phase, the component molar fractions in each phase are given by

$$\begin{cases} c_e^l = \dfrac{H_a - p^g}{H_a - \widetilde{p}_{sat}}, \qquad c_a^l = \dfrac{p^g - \widetilde{p}_{sat}}{H_a - \widetilde{p}_{sat}}, \\ \\ c_e^g = \dfrac{\widetilde{p}_{sat}}{p^g} c_e^l, \qquad c_a^g = \dfrac{H_a}{P^g} c_a^l, \end{cases}$$

with the vapor pressure $p_{sat}(T) = 1.013\ 10^5 e^{13.7 - 5120/T}$ Pa, the Henry constant $H_a = 6\ 10^9$ Pa, and $\widetilde{p}_{sat} = p_{sat}(T) e^{\frac{p^l - p^g}{\zeta^l RT}}$ Pa.

The phase viscosities are fixed to $\mu^g = 18.51\ 10^{-6}$ Pa.s^{-1} and $\mu^l = 10^{-3}$ Pa.s^{-1}. The Darcy Forchheimer parameters are set to $\alpha = 0$ and $\beta = 10^{-3}$ Kg.m^{-4}. The relative permeabilities and capillary pressure are given by the following Van-Genuchten laws

$$k_r^l(s^l) = \begin{cases} 0 & \text{if} \quad s^l < s_r^l, \\ 1 & \text{if} \quad s^l > 1 - s_r^g, \\ \sqrt{\bar{s}^l}\Big(1 - (1 - (\bar{s}^l)^{1/m})^m\Big)^2 & \text{if} \quad s_r^l \le s^l \le 1 - s_r^g, \end{cases}$$

$$k_r^g(s^g) = \begin{cases} 0 & \text{if} \quad s^g < s_r^g, \\ 1 & \text{if} \quad s^g > 1 - s_r^l, \\ \sqrt{1 - \bar{s}^l}\Big(1 - (\bar{s}^l)^{1/m}\Big)^{2m} & \text{if} \quad s_r^g \le s^g \le 1 - s_r^l, \end{cases}$$

and

$$s^l(p_c) = s_r^l + (1 - s_r^l - s_r^g) \frac{1}{\Big(1 + (\frac{p_c}{P_r})^n\Big)^m},$$

with

$$\bar{s}^l = \frac{s^l - s_r^l}{1 - s_r^l - s_r^g}.$$

Two different rocktypes are considered in the matrix domain $\Omega \setminus \overline{\Gamma}_f$. For $r_S < r < r_I = 3$ m we consider a damaged rock with isotropic permeability $\mathbf{K}_m = 5\ 10^{-18}$ m^2 and a porosity $\phi_m = 0.15$, and for $r > r_I$ we consider the Callovo-Oxfordian argillites (COx) with the same porosity $\phi_m = 0.15$ and the anisotropic permeability defined by $\mathbf{K}_m = \begin{pmatrix} \lambda & 0 & 0 \\ 0 & \lambda & 0 \\ 0 & 0 & \frac{\lambda}{10} \end{pmatrix}$ with $\lambda = 5\ 10^{-20}$ m^2 in the x, y, z Cartesian coordinates where z is the vertical coordinate and x the direction of the Gallery. The Van-Genuchten parameters are defined by $n = 1.50$, $s_r^l = 0.2$, $s_r^g = 0$, $P_r = 5\ 10^6$ Pa in the damaged zone, and by $n = 1.49$, $s_r^l = 0.4$, $s_r^g = 0$, $P_r = 15\ 10^6$ Pa in the COx region. In the fracture Γ_f, the fracture width is equal to $d_f = 0.01$ m, the porosity is set to $\phi_f = 0.3$, the permeability is isotropic and set to $\mathbf{K}_f = 10^{-13}$ m^2, and The Van-Genuchten parameters are defined by $n = 4$, $s_r^l = 0$, $s_r^g = 0$, $P_r = 5\ 10^5$ Pa.

The porous medium is initially saturated by the liquid phase with imposed pressure $p_{ini}^l = 40\ 10^5$ Pa and composition $c_{a,ini}^l = 0$, $c_{e,ini}^l = 1$. At the external boundary $r = r_\omega$ the water pressure is fixed to $\bar{p}^l = p_{ini}^l$, with an input composition $\bar{c}_a^l = 0$, $\bar{c}_e^l = 1$. At both sides $x = 0$ and $x = L$ of the porous medium, zero flux boundary conditions are imposed. The initial condition in the gallery is given by $p_{ini} = 10^5$ Pa and $c_{e,ini}$ defined by the relative humidity

$$H_{r,ini} = \frac{c_{e,ini} p_{ini}}{p_{sat}(T)} = 0.5.$$

We consider an input gas velocity $w_{in} = 1$ m.s^{-1}, a fixed input water molar fraction $\bar{c}_{e,0} = c_{e,ini}$ at the left side $x = 0$ of the gallery, and a fixed output pressure $\bar{p}_L = p_{ini}$ at the right side $x = L$ of the gallery. The simulation is run over a period of 20000 days with an initial time step of 0.1 seconds and a maximum time step of 1000 days.

At the opening of the gallery at $t = 0$, we observe in Figure 3 an increase of the mean relative humidity up to say 0.98 in a few seconds due to a large liquid flow rate at the interface. Then, the flow rate decreases and we observe a drying of the gallery due to the ventilation at $w_{in} = 1$ m.s^{-1} down to an average relative humidity slightly above $H_{r,ini}$ in a few tens days. Meanwhile the gas penetrates slowly into the porous medium reaching a stationnary state with around 160 m^3 of gas in say 10000 days (see Figure 2). As can be seen in Figure 1, the gas penetrates much deeper and at a much higher saturation in the fracture than in the porous medium due to the higher permeability and to the lower capillary pressure in the fracture than in the porous medium.

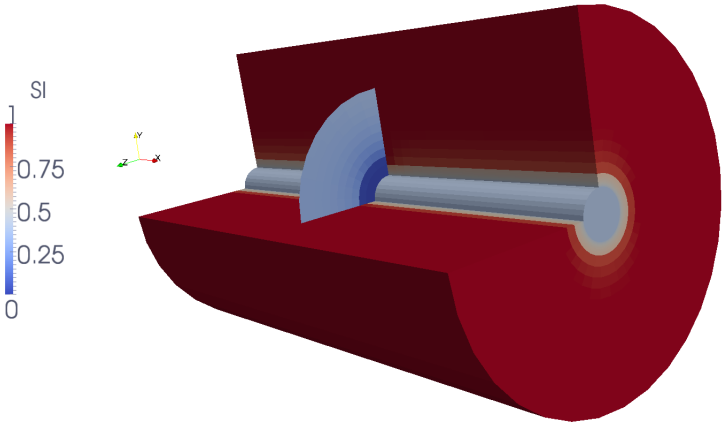

Figure 1: One fracture test case: liquid saturation s^l at the end of the simulation. In the gallery the liquid saturation corresponds to the saturation at the interface as a function of x.

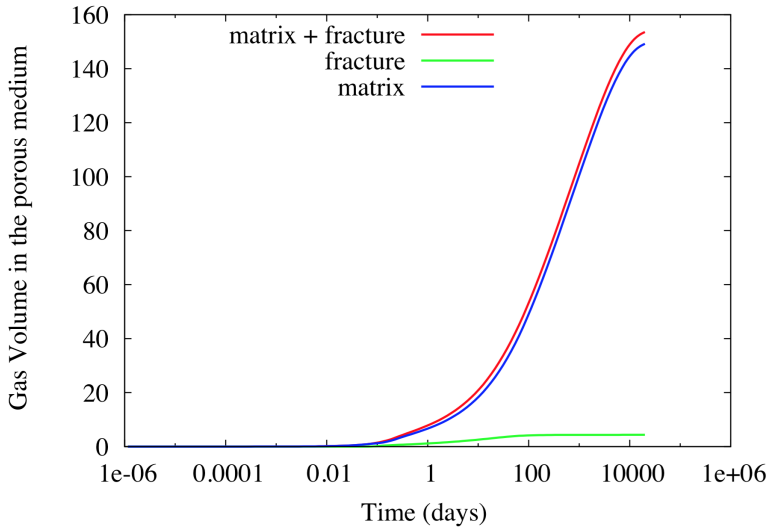

Figure 2: One fracture test case: volume of gas in the matrix, in the fracture and in the porous medium (matrix + fracture) as a function of time.

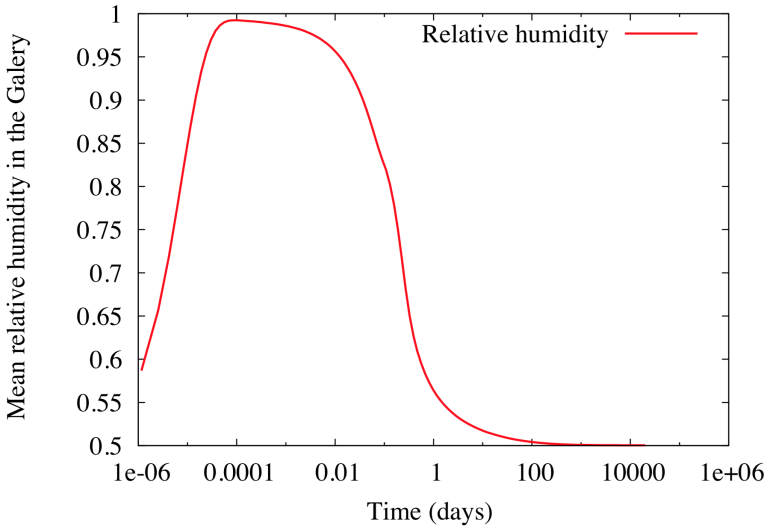

Figure 3: One fracture test case: mean relative humidity in the gallery as a function of time (equal to 0.5 at initial time).

4.2 Test case with 4 fractures

We consider the same test case than the previous one but including 4 fractures defined by $x = 35$ m, $\theta \in [0, 2\pi)$, $r \in (r_S, r_f)$ for the first fracture, by $x = 65$ m, $\theta \in [0, 2\pi)$, $r \in (r_S, r_f)$ for the second fracture, by $\theta = \frac{\pi}{4}$, $r \in (r_S, r_f)$, $x \in (25, 75)$ for the third one, and by $\theta = \frac{5\pi}{4}$, $r \in (r_S, r_f)$, $x \in (25, 75)$ for the last one. The numerical results exhibited in Figures 4, 5, 6 are similar to those of the previous test case with, as expected, a larger amount of gas in the fracture network, and a slightly higher relative humidity in the transient phase.

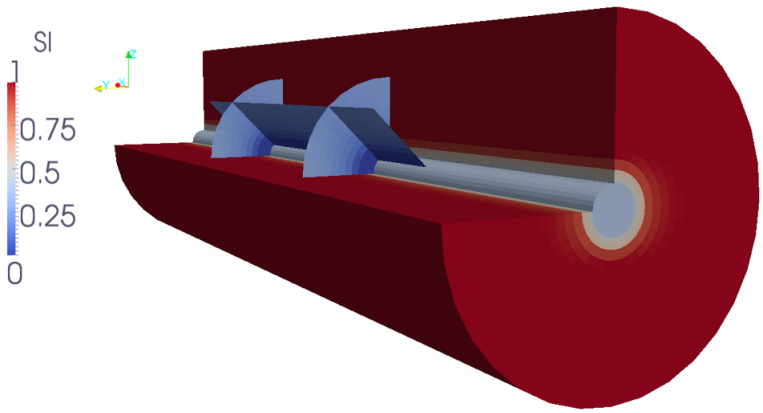

Figure 4: Four fractures test case: liquid saturation s^l at the end of the simulation. In the gallery the liquid saturation corresponds to the saturation at the interface as a function of x.

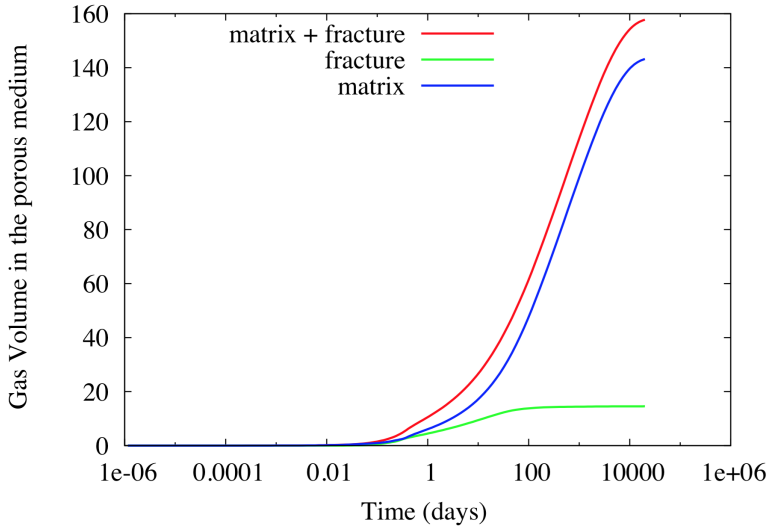

Figure 5: Four fractures test case: volume of gas in the matrix, in the fracture and in the porous medium (matrix + fracture) as a function of time.

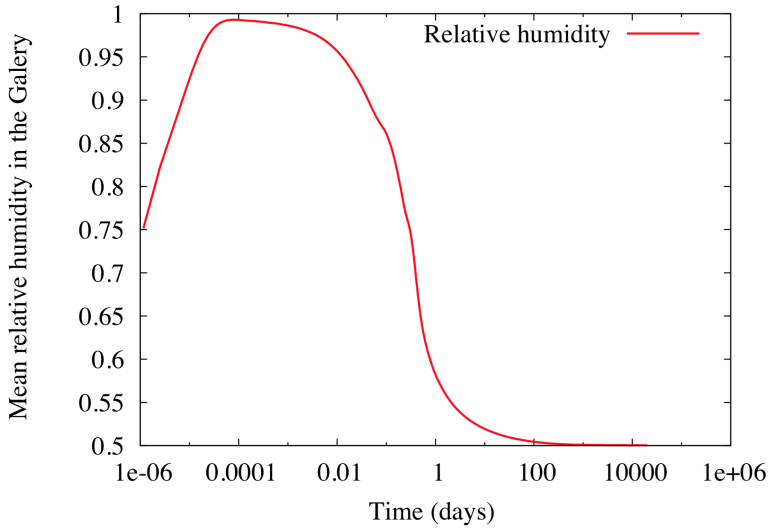

Figure 6: Four fractures test case: mean relative humidity in the gallery as a function of time (equal to 0.5 at initial time).

5 Conclusion

A reduced model coupling the 3D gas liquid compositional Darcy flow in the matrix, the 2D compositional gas liquid Darcy flow in the fracture network, and a 1D compositional gas free flow has been proposed and applied to predict the mass exchanges occuring at the interface between the repository and the ventilation excavated galleries. This reduced model is formulated using the single set of unknowns corresponding to the gas and liquid pressures in the two components case. Then, the VAG scheme is extended to the discretization of such model using a 1D finite element mesh in the gallery non necessarily matching with the mesh of the porous medium. This scheme has the advantage compared with classical CVFE approaches to avoid the mixing of highly contrasted properties inside the control volumes at the nodes located at the interfaces

between on the one hand the fracture and the matrix as well as on the other hand between the gallery and the porous medium. The numerical results on test cases including 1 and 4 fractures exhibit the good physical behavior of the model.

Acknowledgements: the authors would like to thank Andra for its financial support and for allowing the publication of this work.

References

[1] Alboin C., Jaffré J., Roberts J., Serres C. (2002). Modeling fractures as interfaces for flow and transport in porous media. In: Chen, Ewing, editors. Fluid flow and transport in porous media, 295 AMS, 13-24.

[2] Angelini O., Chavant C., Chénier E., Eymard R., Granet S. (2011). Finite volume approximation of a diffusion-dissolution model and application to nuclear waste storage. Mathematics and Computers in Simulation, 81(10), 2001-2017.

[3] Baber K., Mosthaf K., Flemisch B., Helmig R., Müthing S. (2012). Numerical scheme for coupling two-phase compositional porous-media flow and one-phase compositional free flow. IMA Journal of Applied Mathematics, 77(6).

[4] Bourgeat A., Jurak M., Smai F. (2009). Two phase partially miscible flow and transport in porous media; application to gas migration in nuclear waste repository. Computational Geosciences, 13(1), 29-42.

[5] Brenner K., Groza M., Guichard C., Masson R. (2014). DOI web-page: http://dx.doi.org/10.1051/m2an/2014034. Vertex approximate gradient scheme for hybrid dimensional two-phase darcy flows in fractured porous media. M2AN.

[6] Brenner K., Masson R. (2013). Convergence of a vertex centred discretization of two-phase darcy flows on general meshes. International Journal of Finite Volume, june.

[7] Discacciati M., Miglio E., Quarteroni A. (2002). Mathematical and numerical models for coupling surface and groundwater flows. Appl. Num. Math., 43.

[8] Eymard R., Herbin R., Guichard C., Masson R. (2012). Vertex centred discretization of compositional multiphase darcy flows on general meshes. Comp. Geosciences, 16, 987-1005.

[9] Eymard R., Guichard C., Herbin R., Masson R. (2013).DOI web-page: 10.1002/zamm.201200206. Gradient schemes for two-phase flow in heterogeneous porous media and Richards equation. ZAMM - Journal of Applied Mathematics and Mechanics.

[10] Eymard R., Guichard C., Herbin R. (2010). Small-stencil 3d schemes for diffusive flows in porous media. ESAIM: Mathematical Modelling and Numerical Analysis, 46, 265-290.

[11] Helmig R., Flemisch B., Wolff M., Ebigbo A., Class H. (2013). Model coupling for multiphase flow in porous media. Advances in Water Resources, 51.

[12] Masson R., Trenty L., Zhang Y. (2014). Formulations of two-phase liquid gas compositional Darcy flows with phase transitions. International Journal of Finite Volume.

[13] Mosthaf K., Baber K., Flemisch B., Helmig R., Leijnse A., Rybak I., Wohlmuth B. (2011). A coupling concept for two-phase compositional porous-medium and single-phase compositional free flow. Water Resources Research, 47(10).

[14] Tran Q. H., Ferre D., Pauchon C. and Masella J. P. (1998). DOI web-page: http://dx.doi.org/10.2516/ogst:1998070. Transient Simulation of Two-Phase Flows in Pipes. Oil & Gas Science and Technology, 53(6), 801-811.